

Excitation spectrum for an inhomogeneously dipole-field-coupled superconducting qubit chain

Hou Ian,^{1,2} Yu-xi Liu,^{1,3,4} and Franco Nori^{1,5}

¹Advanced Science Institute, RIKEN, Wako-shi, Saitama 351-0198, Japan

²Faculty of Science and Technology, University of Macau, Macau

³Institute of Microelectronics, Tsinghua University, Beijing 100084, China

⁴Tsinghua National Laboratory for Information Science and Technology (TNList), Tsinghua University, Beijing 100084, China

⁵Physics Department, The University of Michigan, Ann Arbor, MI 48109, USA

When a chain of N superconducting qubits couples to a coplanar resonator in a cavity, each of the qubits experiences a different dipole-field coupling strength due to the waveform of the cavity field. We find that this inhomogeneous coupling leads to a dependence of the qubit chain's ladder operators on the qubit-interspacing l . Varying the spacing l changes the transition amplitudes between the angular momentum levels. We derive an exact diagonalization of the general N -qubit Hamiltonian and, through the $N = 4$ case, demonstrate how the l -dependent operators lead to a denser one-excitation spectrum and a probability redistribution of the eigenstates. Moreover, we show that the variation of l between its two limiting values coincides with the crossover between Frenkel- and Wannier-type excitons in the superconducting qubit chain.

PACS numbers: 02.20.Qs, 03.65.Fd, 42.50.Ct, 85.25.-j

I. INTRODUCTION

Superconducting quantum circuits have attracted considerable attention because of their capabilities (i) to demonstrate macroscopically the basic interaction of one “atom” and one photon in a cavity (e.g., [1, 2]), (ii) to serve as a platform for testing many quantum optical phenomena (e.g., [3–7]), as well as (iii) to show its potential as a basis for quantum information processing (e.g., [8–11]).

While research on single-qubit interactions are more common, many recent articles also studied multi-qubit interactions. Superconducting circuits with such interactions are also known as quantum metamaterials [12]. To be precise, the circuit system we consider here consists of a chain of N superconducting two-level qubits coupled to a photon mode in a superconducting coplanar waveguide resonator. Compared to the single-qubit version, it can manifest even more quantum phenomena, including plasma waves [13], controllable collective dressed states [14], and quantum phase transitions [15–18]. It also promises potential for various applications, including quantum simulators [19] and quantum memories [20].

Theoretical studies of multi-qubit interactions with a photon often employ the Dicke model [21], where the Pauli operators are summed and transformed into a bosonic operator. In this approach, the chain of qubits is treated collectively as an atomic ensemble and the excited qubits are collectively regarded as one exciton mode. This theoretical simplification proves adequate when (i) the number of excitations in the system is low (in the so-called “one-photon” processes) and (ii) the number of qubits is large enough such that the interspacing L_q between neighboring qubits can be ignored compared to the photon wavelength L_p in the resonator (i.e., the qubits can be regarded as a continuum).

However, the question of how excitations arise in superconducting metamaterials when these two conditions are *not* met remains unanswered. In a realistic setting for a superconducting circuit, the number N of qubits present can range from one to, say, 10, but N would not be as large as the number of atoms we usually have for an alkaline atomic ensemble in

an optical microcavity, which is typically greater than 10^5 . Therefore, the Dicke model, which treats $N \rightarrow \infty$, does *not* apply well to the case of multi-qubit superconducting circuits with $N \leq 10$.

When a chain of superconducting circuit qubits is arranged as a one-dimensional array (i.e., a superconducting qubit chain or SQC), each qubit is *inhomogeneously coupled* to the circuit photon mode. In other words, each qubit has a *different* coupling strength to the traversing photon field. This occurs naturally since, unlike its optical cavity QED counterpart, the photon wavelength L_p is comparable to the qubit interspacing L_q in a superconducting circuit. The coupling strength thus depends on the position of the qubit relative to the photon waveform. The effect of the varying coupling strength becomes even more obvious if multi-mode couplings are taken into consideration. For example, the qubits on the antinodes of the waveform will couple most strongly, whereas those on the nodes will not couple.

The first step to understand and characterize this inhomogeneously-coupled system (the aim of this article) is to obtain the energy spectrum of the collective excitation mode in the chain of qubits and to compare it with that of the Dicke model. We find that the inhomogeneity of the couplings incurs an algebraic deformation of the Pauli operators of the qubits [22–25]. We quantify this deformation through a “deformation factor,” which is a function of the relative spacing $l = 2L_q/L_p$, and characterize the amount the inhomogeneous system deviates from the homogeneous case. The deformation factor modifies the spin operators of the collective qubit chain. Consequently, the excitation spectrum will not only be a function of the eigenenergy of the photon mode and the qubit level spacing, but is also highly related to the deformation factor and hence the relative spacing l .

Note that when atoms are confined to a cavity, the magnetic or laser field that is exerted on them is *uniform*. The strength of the interaction can be uniformly increased or decreased according to the density of the atoms. This macroscopic viewpoint does not differentiate between the identities of the atoms. However, for circuit QED, the identities of the

qubits are partially differentiated since the qubits can be categorized according to the values of their coupling strength to the photon mode. This partial differentiation has made understanding the inhomogeneous system a many-body physics question.

Our deformation algebraic approach here is a statistical approximation method that can be regarded as finding the average contribution of the coupling strength given by the SQC as a whole. In the end, the characterization (the excitation spectrum) of the SQC as an inhomogeneous system is not parametrized by the individual qubits, but by the relative spacing l . In other words, the spacing l is one extra degree of freedom peculiar to the inhomogeneous SQC, not seen in a homogeneous optical cavity.

We will first introduce the model and derive the deformation factor in Sec. II. With the deformation factor, new operation rules for the spin angular momentum operators are found by solving a difference equation in Sec. III. The general energy spectrum for n -qubit SQC is given in Sec. IV. We also derive in Sec. IV a one-excitation spectrum for a 4-qubit SQC as a nontrivial case to show the effects of the inhomogeneity. Namely, the energy splittings between the eigenstates of the deformed coupling case shrink, while the probability amplitudes of the eigenstates are redistributed such that higher-photon occupations are favored.

In the final Sec. V, we will consider how the collective excitations on the SQC would emulate the excitons in atomic lattices. In one limit, it becomes a Wannier-type exciton [26], where the wave function of the excited level is localized on a single atom. In the opposite limit, it emulates a Frenkel-type exciton, which has an extended wave function across multiple atoms. Changing the degree of freedom l lets the emulated exciton undergo a crossover between these two types of excitons. This crossover depends on a $(2N - 1)$ -th order trigonometric equation, whose solution corresponds to the asymptotic turning point from the deformed (inhomogeneously-coupled) SQC to the undeformed (homogeneously-coupled) SQC.

II. INHOMOGENEOUS COUPLING MODEL

A. Inhomogeneous coupling

For a finite number N of spins in the SQC, the problem discussed here is similar to the Tavis-Cummings (TC) model [27, 28], where all the spins are grouped into a total “large” spin. However, the exactly solvable TC model applies only when the coupling is homogeneous and when the eigenfrequencies between the qubits and the photon mode are equal. When the coupling is inhomogeneous, the large spin does not obey the usual commutation relations of the Pauli matrices, which the TC-model assumes.

The new commutation relations of the large spin introduced by the inhomogeneity are pertinent to the deformed SU(2) Lie algebras. From these algebraic structures, we can establish a deformed dipole-field coupling model, of which the TC model is a special case. In the following discussion, we consider the typical case where the inter-qubit spacing is uniform. The

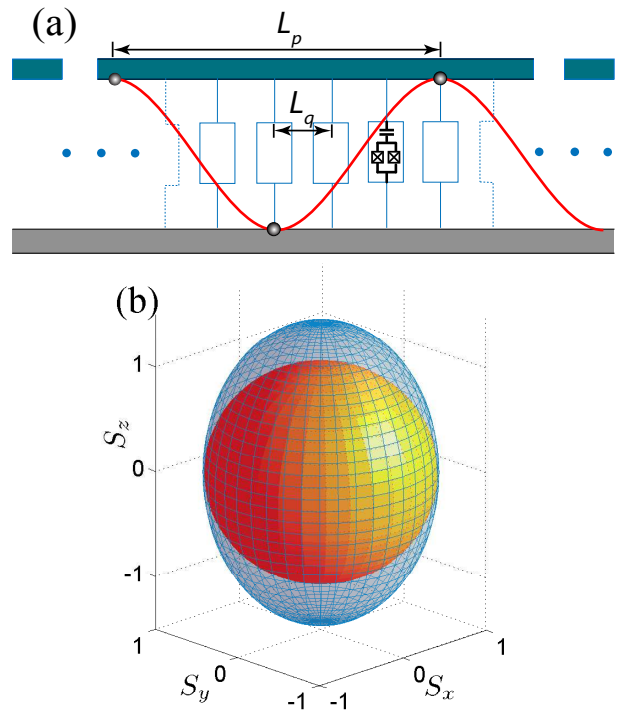


Figure 1: (Color online) (a) Schematic diagram of an SQC with spacing $l = 1/3$. The upper strip represents a coplanar resonator whose potential waveform of wavelength L_p is drawn as a sinusoidal curve, while the lower one represents a ground strip. The rectangles between the strips are qubits with interspacing L_q . The gray dots on the curve indicate the anti-nodes of the waveform. (b) The elongation effect on the large spin due to inhomogeneous coupling. The ellipsoid shows a case of deformation $R_{N,l} = 0.5$. The unit sphere shows the spin under the usual homogeneous coupling.

coupling strength of each qubit to the photon field can, therefore, be written as a cosine function of a phase factor which is determined by the position jl of the j -th qubit, where j is the reduced coordinate and l is the relative spacing introduced above.

The situation is illustrated in Fig. 1(a). A chain of qubits is sandwiched between the superconducting coplanar resonator and a superconducting ground strip. The photon mode providing different potential energies on the spins is shown by the red sinusoidal curve.

We use the operators $\{\sigma_{j,z}\}$ to denote Josephson junction qubits, and $\{a, a^\dagger\}$ to denote the operators for the single-photon mode. With the wave vector being the reciprocal of the photon field wavelength on the one-dimensional lattice, $k = 2\pi/L_p$, the dipole-field coupling is of the form $\sigma_{j,x}(a \cos(j\pi l) + \text{h.c.})$. Under the rotating wave approximation, the Hamiltonian can be written as ($\hbar = c = 1$)

$$H = \omega_q \sum_{j=0}^{N-1} \sigma_{j,z} + \omega_0 a^\dagger a + \eta \sum_{j=0}^{N-1} \cos(j\pi l) [\sigma_{j,+} a + \sigma_{j,-} a^\dagger] \quad (1)$$

where ω_q is the eigenenergy of the spins, ω_0 the mode frequency of the photon, and η the coupling amplitude.

To diagonalize the Hamiltonian in Eq. (1), we introduce the

“large spin” operators: the magnetic moment or z -direction collective spin operator

$$S_z = \sum_{j=0}^{N-1} \sigma_{j,z}, \quad (2)$$

which is no different from the homogeneous case, and the paired raising and lowering operators

$$S_+ = \sum_{j=0}^{N-1} \sigma_{j,+} \cos(j\pi l) \quad (3)$$

$$S_- = \sum_{j=0}^{N-1} \sigma_{j,-} \cos(j\pi l) \quad (4)$$

which have the special sinusoidal dependence on l due to the inhomogeneity. The commutator of the paired ladder operators *no* longer equals to $2S_z$ but has an additional term due to the cosine coefficients, i.e., $[S_+, S_-] = 2\Sigma_z$ with

$$\Sigma_z = S_z + \sum_{j=0}^{N-1} \sin[j\pi(1+l)] \sin[j\pi(1-l)] \sigma_{j,z}. \quad (5)$$

The detailed derivation is shown in Appendix A 1. Note that in the usual circuit QED system [2], where only one spin is placed at midway, the spacing l equals to 2, for which the latter term in Σ_z vanishes. This is the limiting case which corresponds to the Wannier type of excitation, where the set of spin operators retains the usual structure of an undeformed SU(2) algebra.

B. Deformed algebraic structure

When the second term of Σ_z does not vanish, the algebraic structure is called deformed [22–25]. In order to quantify the deformation, the commutator of the ladder operators needs to be expressed as a function of S_z , i.e., $\Sigma_z = f(S_z)$. To find this function f , we consider an underlying manifold, on which there is a local point, say the origin 0, where we define a tangent space with the Pauli z -matrices $\{\sigma_{j,z}\}$ being its basis vectors, since these matrices are linearly independent. The operator S_z , defined above with uniform coefficients, can be deemed a vector in this tangent space; the operator Σ_z is then another vector dependent on the parameter l and is a deviation or deformation from S_z . Thus, the first-order approximation of Σ_z with respect to S_z is its projection onto the vector S_z . That is, since the cosine coefficients are bounded, we can use their Hilbert-Schmidt norm

$$\langle \Sigma_z, S_z \rangle = \text{tr}(\Sigma_z^* S_z) = N + \sum_{j=0}^{N-1} \cos(2j\pi l) \quad (6)$$

and the Schmidt decomposition [29] to write $\Sigma_z = R_{N,l} S_z$ as a deformation of the original z -spin operator where

$$R_{N,l} = \frac{1}{4N} \left\{ 2N + 1 + \frac{\sin[(2N-1)\pi l]}{\sin(\pi l)} \right\} \quad (7)$$

is the deformation factor (Cf. Appendix A 2 for this derivation). The commutator of the ladder operators can now be expressed as

$$[S_+, S_-] = 2R_{N,l} S_z, \quad (8)$$

where $R_{N,l}$ has a limiting value of one when $l \rightarrow 0$ or $l \rightarrow \infty$, for which the usual structure used in the TC model is retained.

Since the deformation factor $R_{N,l}$ does not affect the commutation relations between the ladder operators and the z -spin, the large-spin operators $\{S_z, S_+, S_-\}$ form a specific deformed algebra [22, 23] and not the more general type [24]. The Casimir operator

$$C = S_- S_+ + h(S_z) \quad (9)$$

of the algebra, which equals to the undeformed spin momentum square, $S^2 = S_x^2 + S_y^2 + S_z^2$, for the homogeneous coupling case, is accordingly deformed. Through solving a recursive relation (Cf. Appendix A 3 for details), we find $h(S_z) = R_{N,l}(S_z^2 + S_z)$ and hence

$$C = S_x^2 + S_y^2 + R_{N,l} S_z^2, \quad (10)$$

which shows that the spin momentum is *reduced* along the z -direction:

$$S^2 = S_x^2 + S_y^2 + R_{N,l} S_z^2. \quad (11)$$

To visualize this reduction of the spin momentum, we can take a unit value for the spin moment and let the Casimir operator be represented by a unit sphere in 3-dimensional space for the undeformed case. With $R_{N,l} \leq 1$, the deformation would be an elongation of the unit sphere, along the z -axis, to an ellipsoid, while the x - and y -semi-minor axes remain unchanged, as shown in Fig. 1(b).

III. OPERATION RULES

If we consider the unit sphere of Fig. 1(b) as a Bloch sphere on which the large spin prescribes its N levels, its elongation due to deformation will accordingly modify the transitions between the levels. Since the spin-up and the spin-down momenta do not change, which are still $\omega_q N/2$ and $-\omega_q N/2$, the narrow part of the ellipsoid effectively squeezes the transition probabilities.

More precisely, we consider an arbitrary eigenstate $|r, m\rangle$, for which

$$S_z |r, m\rangle = m |r, m\rangle \quad (12)$$

$$S^2 |r, m\rangle = r(r+1) |r, m\rangle. \quad (13)$$

The ladder operators result in an (r, m) -dependent off-diagonal matrix element $\alpha_m^{(r)}$, i.e.,

$$S_+ |r, m\rangle = \alpha_m^{(r)} |r, m+1\rangle \quad (14)$$

$$S_- |r, m\rangle = \alpha_{m-1}^{(r)} |r, m-1\rangle \quad (15)$$

By examining the diagonal elements of the commutator of the ladder operators, we find a difference equation $(\alpha_m^{(r)})^2 - (\alpha_{m-1}^{(r)})^2 = -2mR_{N,l}$. With the value $\alpha_{-r}^{(r)} = 0$, the equation can be solved to give the deformed off-diagonal matrix elements or transition probabilities for the ladder operators

$$\alpha_m^{(r)} = \sqrt{R_{N,l}(r-m)(r+m+1)}. \quad (16)$$

See Appendix B for its derivation.

Geometrically speaking, the deformation process is a homeomorphism with a redefined metric $g = (1, 1, R_{N,l})$. Since $R_{N,l} \leq 1$, the metric norm is less than unity. The deformation does not affect the level spacings of the magnetic moment S_z : the number m still takes $(2r+1)$ values (i.e., the ellipsoid is homeomorphic to the sphere). But the transition amplitudes to traverse the sphere decrease: if we start with a spin-up state $|r, r\rangle$ and finish with a spin-down state $|r, -r\rangle$, then all iterations with $S_-|r, m\rangle = \alpha_{m-1}^{(r)}|r, m-1\rangle$ have $\alpha_m^{(r)}$ smaller than the original $\bar{\alpha}_m^{(r)} = \sqrt{(r-m)(r+m+1)}$ (i.e., the ellipsoid is not isometric to the sphere).

The deformation factor expressed in Eq. (7) is an oscillating function of l , where the sine in the numerator determines the period of oscillation and the sine in the denominator determines the period of the envelope. Therefore, the spin angular momentum of the SQC would be *oscillating* between the unit sphere and the ellipsoid, depending on the qubit spacing l . The plot of $R_{N,l}$ in Fig. 2(a) for an SQC of $N = 30$ qubits shows a typical case with envelop of period 1 and local minimum of 0.4. The function $h(S_z)$ associated with this deformation factor is a parabola of the magnetic moment S_z . For a nontrivial deformation $R_{N,l} < 1$, this parabola flattens and the spin levels become denser. The curvature of the parabola decreases while its minimum value $-R_{N,l}/4$ increases. As shown in Fig. 2(b), the black (gray) arrow indicates the spin level $r = 1/2$ for the deformed $R_{N,l} = 0.4$ (undeformed $R_{N,l} = 1$) case of SQC. So varying l makes the curve $h(S_z)$ oscillate between the boldened curves that correspond to $R_{N,l} = 0.4$ and $R_{N,l} = 1$, respectively. We can also observe that the level splittings are reduced, reflecting the elongated structure of the Bloch sphere in Fig. 1(b) and the modified operation rule of Eq. (16).

IV. DEFORMED SPECTRUM

Equipped with the modified operation rules, we can diagonalize the Hamiltonian in Eq. (1). First, we split the Hamiltonian into two parts

$$H_0 = \omega_0(S_z + a^\dagger a), \quad (17)$$

$$H_1 = \tilde{\omega}_0 a^\dagger a + \eta(S_+ a + S_- a^\dagger). \quad (18)$$

Let u be the number of total excitations and hence the eigenvalue of H_0 . Let n be the number of photons in the system such that the SQC magnetic moment is $m = u - n$. Let ν be the eigenvalue of the interaction part H_1 , where $\tilde{\omega}_0 = \omega_0 - \omega_q$.

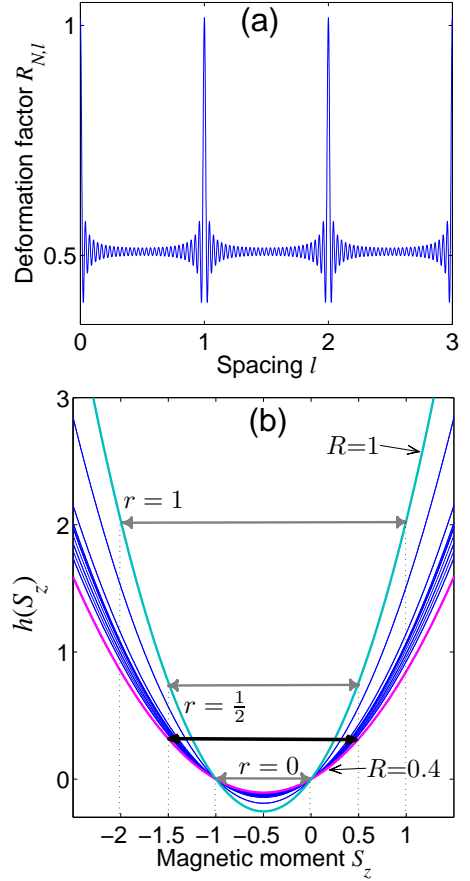


Figure 2: (Color online) (a) The deformation factor $R_{N,l}|_{N=30}$, as an oscillating function of the qubit spacing l . (b) Plot of the function $h(S_z)$ for various values of $R_{N,l}$. The top and bottom boldened curves correspond to $R_{N,l} = 1$ and 0.4 , respectively. The gray-shaded double-arrows indicate three spin levels of the undeformed SQC, while the black arrows show the $r = 1/2$ level of the deformed case.

The eigenvector of the Hamiltonian can then be expanded as a superposition of different configurations of photon number and spin states:

$$|u, r\rangle = \sum_n c_n |n; r, u-n\rangle. \quad (19)$$

The expansion coefficients c_n satisfy a recursive relation [28]:

$$c_{n+1}\sqrt{n+1}\alpha_{u-(n+1)}^{(r)} - c_n\tilde{\nu}_n + c_{n-1}\sqrt{n}\alpha_{u-n}^{(r)} = 0 \quad (20)$$

where $\tilde{\nu}_n = (v - \tilde{\omega}_0 n)/\eta$.

The solution reads

$$c_n = \sum_{p=0}^{\lfloor n/2 \rfloor} (-1)^p (R_{N,l})^{p-n/2} \mathcal{C}_{n,p}. \quad (21)$$

$\mathcal{C}_{n,p}$ can be regarded as a probability amplitude contribution to the n -photon state from a set of corresponding qubit chain

Table I: Configurations $|n; r, m\rangle$ and probability amplitudes c_n for the one-excitation spectrum of an SQC with $N = 4$ qubits and spacing $l = 2/3$. Each \circ indicates one photon while \uparrow or \downarrow denotes the spin state of each qubit. Here, $\tilde{v}_n = (v - \tilde{\omega}_0 n)/\eta$.

$u = 1$ $r = 2$	$n = 0$ $m = 1$	$n = 1$ $m = 0$	$n = 2$ $m = -1$	$n = 3$ $m = -2$
photon	—	○	○○	○○○
spin	↓↑↑↑	↑↑↓↓, ↓↓↑↑	↑↓↓↓	↓↓↓↓
config.	↑↑↑↑	↑↓↑↑, ↓↑↑↓	↓↑↓↓	
	↑↑↑↓	↑↓↑↓, ↓↑↓↑	↓↓↑↓	
	↑↑↓↓	↓↓↑↑		
c_n	1	$\frac{\tilde{v}_0}{\sqrt{6R}}$	$\frac{\tilde{v}_0 \tilde{v}_1}{6\sqrt{2}R} - \frac{1}{\sqrt{2}}$	$\frac{\tilde{v}_0 \tilde{v}_1 \tilde{v}_2}{12\sqrt{6}R^{3/2}} - \frac{\tilde{v}_2 + 2\sqrt{6}\tilde{v}_0}{12\sqrt{R}}$

states indexed by p :

$$\mathcal{C}_{n,p} = \frac{P_n}{\sqrt{n!}} \sum_{\langle j_1 \dots j_k \dots j_{[n/2]} \rangle} \cdots \sum_{k=1}^p \prod_{k=1}^p \frac{(j_k + 1)}{\tilde{v}_{j_k} \tilde{v}_{j_k+1}} \left[\bar{\alpha}_{u-(j_k+1)}^{(r)} \right]^2 \quad (22)$$

where $P_n = \prod_{j=0}^{n-1} \tilde{v}_j / \bar{\alpha}_{u-(j+1)}^{(r)}$ and $\langle j_1 \dots j_k \dots j_{[n/2]} \rangle$ represents an index set of descending order $\{\forall k < l : 0 \leq j_l \leq j_k - 2; 0 \leq j_1 \leq n - 2\}$. We can see from Eq. (21) that the operation rules discussed in the preceding paragraphs have made the probability amplitudes deformation-dependent, thus l -dependent. This will consequently lead to a redistribution of probabilities for different photon states. See Appendix C 1 for the derivation of these coefficients $\mathcal{C}_{n,p}$.

The simplest nontrivial example of this deformation effect can be seen in Table. I, where we consider the one-excitation ($u = 1$) spectrum of a four-qubit SQC with spacing $l = 2/3$. The deformation factor in this case is $R_{N,l} = 5/8$. For a weakly coupled SQC with $|\tilde{\omega}_0| \gg \eta$, the eigenenergies for the four levels are given by (Cf. Appendix C 2 for the derivation)

$$E_{\pm, \pm} = \omega_q + \frac{3}{2} \tilde{\omega}_0 \pm \frac{1}{2} \left[5\tilde{\omega}_0^2 \pm 4\tilde{\omega}_0 (\tilde{\omega}_0^2 + 36R_{N,l}\eta^2)^{1/2} \right]^{1/2}. \quad (23)$$

For a deformation factor $R_{N,l} < 1$, the splittings between these dressed levels are suppressed. In addition, if we substitute the value of v into the coefficients c_n , we will find that c_1 is greater than that of the undeformed case, c_2 (c_3) increases by a greater proportion than c_1 (c_2), while c_0 remains equal to one. Therefore, the probability distribution shifts toward the end that favors states with greater number of photons and less degeneracy.

V. EXCITON CROSSOVER

If the spacing l is large ($L_q \gg L_p$), i.e., there are multiple photon wavelengths between two neighboring qubits, we can consider the excitation that the dipole-field coupling induces on a qubit to be localized on that qubit. Consequently, this type of excitation emulates the Wannier exciton on an atomic lattice. If l is small ($L_q \ll L_p$) with a single-photon wavelength extending over all the qubits, we can consider the excitation on the SQC to be delocalized. This type of excitation

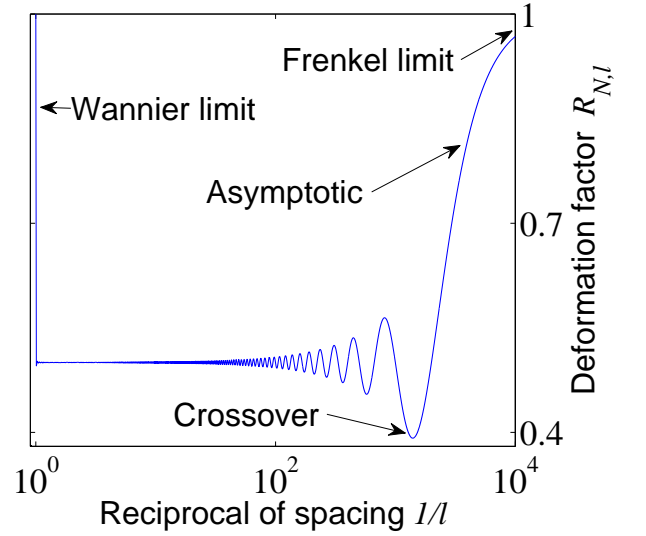


Figure 3: Semi-log plot of the deformation factor $R_{N,l}$ versus $1/l$ over one period, showing the Wannier limit on the left end and the Frenkel limit on the right end of the horizontal axis. The number of qubits is set to $N = 1000$.

emulates the Frenkel's exciton model for molecular crystals. Note that when l tends to either zero or infinity in Eq. (5), Σ_z falls back to S_z and the regular $SU(2)$ algebra for the commutators is obtained. Thus, it is justified that in the large- N limit, the low-energy excitation becomes bosonic for both Wannier and Frenkel excitons.

To determine when the emulated exciton crosses from Wannier- to Frenkel-type, we plot in Fig. 3 the deformation factor versus the reciprocal of the spacing over $10^{-4} < l < 1$, where we can see the asymmetry between the left edge ($1/l \rightarrow 0$) for the Wannier limit and the right edge ($1/l \rightarrow \infty$) for the Frenkel limit. Setting $dR_{N,l}/dl = 0$, we obtain the trigonometric equation

$$\tan[(2N - 1)\pi l] = (2N - 1) \tan(\pi l). \quad (24)$$

Transforming Eq. (24) to $U_{2N-1}(\cos \pi l) = 2N \cdot T_{2N-1}(\cos \pi l)$, where T_{2N-1} (U_{2N-1}) is the Chebyshev polynomial of the first (second) kind, we can observe that it is a $(2N - 1)$ -th order polynomial equation. Hence, the curve has $(2N - 1)$ local extrema in exactly $(N - 1)$ oscillations from the Wannier end to the asymptotic Frenkel end. Between these two limits, the excitation has various degrees of deformation and the crossover is continuous. We can regard the crossover point to be the absolute minimum before the deformation factor asymptotically approaches one. This point approaches 0 when $N \rightarrow \infty$. For the case illustrated in Fig. 3 with $N = 1000$, a numerical estimation gives the crossover at $l = 7.16 \times 10^{-4}$, or a length of 2800 spins per photon wavelength.

VI. CONCLUSION

We have studied the inhomogeneous coupling between a SQC and a superconducting coplanar resonator, which leads to a set of deformation-dependent operation rules of spin momentum. The modified rules correspond to tighter energy spacings and a shift of the probability distribution of spin levels. The inhomogeneous coupling also gives rise to different types (Frenkel and Wannier) of collective excitations on the SQC and the crossover between these types is determined by a polynomial equation of the qubit spacing l .

FN acknowledges partial support from LPS, NSA, ARO, DARPA, AFOSR, NSF grant No. 0726909, JSPSRFBR contract No. 09-02-92114, MEXT Kakenhi on Quantum Cybernetics, and Funding Program for Innovative R&D on S&T. YXL acknowledges support from the NNSFC grant No. 10975080 and 61025022.

Appendix A: Derivation of the deformation factor

1. Commutation relation

The commutator of the ladder operators can be computed as follows

$$\begin{aligned} [S_+, S_-] &= \sum_{j,k=0}^{N-1} \cos(j\pi l) \cos(k\pi l) [\sigma_{j,+}, \sigma_{k,-}] \\ &= 2 \sum_{j=0}^{N-1} \cos^2(j\pi l) \sigma_{j,z} \\ &= S_z + \sum_{j=0}^{N-1} \cos(2j\pi l) \sigma_{j,z}. \end{aligned}$$

To use a consistent notation, we write the R.H.S. as $2\Sigma_z$ and extract S_z from the second term

$$\begin{aligned} 2\Sigma_z &= 2S_z + \sum_{j=0}^{N-1} [\cos(2j\pi l) - \cos(2j\pi)] \sigma_{j,z} \\ &= 2S_z + 2 \sum_{j=0}^{N-1} \sin[j\pi(1+l)] \sin[j\pi(1-l)] \sigma_{j,z} \end{aligned}$$

which gives Eq. (5).

We can also check that other commutation relations are preserved

$$\begin{aligned} [S_z, S_\pm] &= \sum_{j,k=0}^{N-1} [\sigma_{k,z}, \sigma_{j,\pm} \cos(j\pi l)] \\ &= \sum_{j=0}^N \pm \sigma_{j,\pm} \cos(j\pi l) \\ &= \pm S_\pm, \end{aligned}$$

from which we conclude that the newly defined operators $\{S_z, S_+, S_-\}$ form a Polychronakos-Rocek type of deformed $SU(2)$ algebra.

2. Deformation factor

First, we recognize that each qubit $\sigma_{j,z}$ has two orthonormal basis vectors $\{|e_j\rangle, |g_j\rangle\}$ for a fixed relative coordinate j and hence $\{|\epsilon_k\rangle : |\epsilon_k\rangle \in \{|e_j\rangle, |g_j\rangle, j = 0, \dots, N-1\}\}$ forms an orthonormal basis for the Hilbert space \mathcal{H} that spans all the qubits on the chain. Then S_z for the original spin angular momentum and Σ_z for that of the inhomogeneous SQC become operators on this Hilbert space \mathcal{H} . Since the sinusoidal functions $\cos(j\pi l)$ are bounded, we can define the Hilbert-Schmidt inner product as

$$\begin{aligned} \langle \Sigma_z, S_z \rangle &= \text{tr}(\Sigma_z^* S_z) = \sum_k^{2N} \langle \epsilon_k | \Sigma_z \cdot S_z | \epsilon_k \rangle \\ &= \sum_k^{2N} \langle \epsilon_k | \sum_{j,l=0}^{N-1} \cos^2(j\pi l) \sigma_{j,z} \cdot \sigma_{l,z} | \epsilon_k \rangle \\ &= \sum_k^{2N} \langle \epsilon_k | \cos^2(\lfloor k/2 \rfloor \pi l) \sigma_{\lfloor k/2 \rfloor, z} \cdot \sigma_{\lfloor k/2 \rfloor, z} | \epsilon_k \rangle \\ &= \sum_k^{2N} \cos^2(\lfloor k/2 \rfloor \pi l) \\ &= \sum_j^N 2 \cos^2(j\pi l) \end{aligned}$$

which equals to Eq. (6). We can then write the approximation of Σ_z as a Schmidt projection on S_z

$$\begin{aligned} \Sigma_z &\approx \frac{\langle \Sigma_z, S_z \rangle}{\langle S_z, S_z \rangle} S_z \\ &= \frac{N+1 + \sum_j \cos(2j\pi l)}{2(N+1)} S_z \\ &= \left[\frac{1}{2} + \frac{1}{2N} \sum_{j=0}^{N-1} \cos(2j\pi l) \right] S_z \\ &= R_{N,l} S_z \end{aligned}$$

where $R_{N,l}$ denotes the deformation factor. Its expression can be further simplified to

$$\begin{aligned} R_{N,l} &= \frac{1}{4N} \left[2N+1 - \cos(2N\pi l) + \frac{\sin(2\pi l) \sin(2N\pi l)}{1 - \cos(2\pi l)} \right] \\ &= \frac{1}{4N} \left[2N+1 - \cos(2N\pi l) + \frac{\cos(\pi l) \sin(2N\pi l)}{\sin(\pi l)} \right] \\ &= \frac{1}{4N} \left[2N+1 + \frac{\sin[(2N-1)\pi l]}{\sin(\pi l)} \right] \end{aligned}$$

where the first line is derived by comparing the real parts in a summation of exponentials.

3. Casimir operator

The Casimir operator for the algebra is

$$C = S_- S_+ + \hbar(S_z)$$

where the second term satisfies a recursive relation [24]

$$h(S_z) - h(S_z - 1) = 2R_{N,l}S_z.$$

This relation leads to a solution composed of Bernoulli polynomials

$$\begin{aligned} h(S_z) &= R_{N,l}(B_2(-S_z) - B_2) \\ &= R_{N,l}(S_z^2 + S_z) \end{aligned}$$

where $B_2(-S_z)$ is the second-order Bernoulli polynomial with the operator S_z as variable and B_2 is the second Bernoulli number. The Casimir operator becomes then

$$\begin{aligned} C &= S_-S_+ + R_{N,l}(S_z^2 + S_z) \\ &= \frac{1}{2}(S_+S_- + S_-S_+) + R_{N,l}S_z^2 \end{aligned}$$

which equals to Eq. (10) and represents a deformed total spin operator S^2 .

Appendix B: Deriving operation rules

Assume the eigenstate of the z -spin momentum operator S_z to be $|r, m\rangle$, that is, $r(r+1)$ denotes the total spin number and m the magnetic moment, for which Eqs. (12)-(13) are satisfied. Further, assume $\alpha_m^{(r)}$ to be the coefficients when the ladder operators are applied to the state vectors as in Eqs. (14)-(15), which is indexed by r and m .

By applying the vector $|r, m\rangle$ to the commutation relation Eq. (8), we find

$$\begin{aligned} \langle r, m | [S_+, S_-] | r, m \rangle &= \langle r, m | S_+S_- - S_-S_+ | r, m \rangle \\ &= (\alpha_{m-1}^{(r)})^2 - (\alpha_m^{(r)})^2 \\ &= \langle r, m | 2R_{N,l}S_z | r, m \rangle \\ &= 2R_{N,l}m. \end{aligned}$$

Selecting the second and the fourth line, we arrive at a difference equation of m :

$$(\alpha_m^{(r)})^2 - (\alpha_{m-1}^{(r)})^2 = -2mR_{N,l}.$$

To solve the equation, we list out the iterations until the last entry where $\alpha_{-r-1}^{(r)} = 0$ since $-r$ is the minimum value m can take as the magnetic moment

$$\begin{aligned} (\alpha_m^{(r)})^2 - (\alpha_{m-1}^{(r)})^2 &= -2R_{N,l}m \\ (\alpha_{m-1}^{(r)})^2 - (\alpha_{m-2}^{(r)})^2 &= -2R_{N,l}(m-1) \\ &\vdots \\ (\alpha_{-r}^{(r)})^2 - (\alpha_{-r-1}^{(r)})^2 &= -2R_{N,l}(-r). \end{aligned}$$

Summing up all the iterations above, we have

$$\begin{aligned} (\alpha_m^{(r)})^2 &= -2R_{N,l} \sum_{j=0}^{m+r} (m-j) \\ &= -R_{N,l}(m-r)(m+r+1), \end{aligned} \quad (\text{B1})$$

which gives Eq. (16). We can verify this result by summing up instead of summing down, i.e., with the condition $\alpha_r^{(r)} = 0$ and the iterations

$$\begin{aligned} (\alpha_m^{(r)})^2 - (\alpha_{m+1}^{(r)})^2 &= 2R_{N,l}(m+1) \\ (\alpha_{m+1}^{(r)})^2 - (\alpha_{m+2}^{(r)})^2 &= 2R_{N,l}(m+2) \\ &\vdots \\ (\alpha_{r-1}^{(r)})^2 - (\alpha_r^{(r)})^2 &= 2R_{N,l}r \end{aligned}$$

we have, after adding them up,

$$\begin{aligned} (\alpha_m^{(r)})^2 &= 2R_{N,l} \sum_{j=0}^{r-m} (m+j) \\ &= R_{N,l}(r-m+1)(m+r), \end{aligned}$$

which is the same as Eq. (B1).

Appendix C: Deriving the excitation spectrum of the superconducting qubit chain

1. State vector compositions for a general N -qubit superconducting qubit chain

The form into which the system Hamiltonian is split as in Eqs. (17)-(18) ensures that $[H_0, H_1] = 0$. The commutation of these two parts implies that we can find simultaneous eigenvectors for H_0 and H_1 .

First, for an eigenvector $|n; r, m\rangle$ (or written as $|u, r\rangle$) of H_0 , we have

$$H_0 |n; r, m\rangle = H_0 |u, r\rangle = \omega_q(m+n) = \omega_q u$$

where $\{u, n, m\}$ assumes meanings as described in Sec. IV. Note that the eigenvalue $\omega_q u$ is degenerate, for different combinations of m and n that add up to the same u . Therefore the eigenstate of H_0 can be written as a superposition

$$\begin{aligned} |u, r\rangle &= \sum_{n,m} c_n |n; r, m\rangle \delta(u-n-m) \\ &= \sum_n c_n |n; r, u-n\rangle \Delta \end{aligned} \quad (\text{C1})$$

where Δ is a range delta function

$$\Delta = \begin{cases} 1, & -r \leq u-n \leq r \\ 0, & \text{otherwise} \end{cases}$$

since we have to ensure the state vectors satisfy the addition rules of angular momentum.

Our next step is to find those of Eq. (C1) that are also simultaneous eigenvectors of H_1 . With the modified operation rule Eq. (16) and setting $m = u - n$, we can apply H_1 to the expression and, after reshuffling the terms in the summation

such that vectors with the same total excitation number are grouped together, we find

$$H_1 |u, r\rangle = \sum_n \left\{ c_n \tilde{\omega}_0 n + c_{n+1} \eta \sqrt{(n+1)} \alpha_{u-n}^{(r)} + c_{n-1} \eta \sqrt{n} \alpha_{u-n}^{(r)} \right\} |n; r, u-n\rangle \Delta. \quad (\text{C2})$$

Since ν is the eigenvalue of H_1 , we have

$$H_1 |u, r\rangle = \nu |u, r\rangle = \sum_n c_n \nu |n; r, u-n\rangle \Delta \quad (\text{C3})$$

Then comparing Eq. (C2) with Eq. (C3), we deduce a difference equation

$$c_{n+1} \eta \sqrt{(n+1)} \alpha_{u-(n+1)}^{(r)} - c_n \tilde{\nu}_n + c_{n-1} \eta \sqrt{n} \alpha_{u-n}^{(r)} = 0$$

where $\tilde{\nu}_n = (\nu - \tilde{\omega}_0 n) / \eta$ and the initial conditions are

$$\begin{aligned} c_{-1} &= 0, \\ c_{u+r+1} &= 0. \end{aligned}$$

In addition, from the definition of the Δ function, $n \leq u+r$. Now write

$$c_n = \frac{C_n}{\sqrt{n!} \prod_{j=1}^n \alpha_{u-j}^{(r)}} \quad (\text{C4})$$

and we have a simplified difference equation

$$C_{n+1} - C_n \tilde{\nu}_n + C_{n-1} n \left(\alpha_{u-n}^{(r)} \right)^2 = 0.$$

To find the solution, we multiply each equation starting with C_j by $\prod_{k=j}^n \tilde{\nu}_k$

$$\begin{aligned} C_n \tilde{\nu}_n - C_{n-1} \tilde{\nu}_n \tilde{\nu}_{n-1} + (n-1) \tilde{\nu}_n C_{n-2} \left[\alpha_{u-(n-1)}^{(r)} \right]^2 &= 0 \\ &\vdots \\ &\vdots \end{aligned}$$

$$\begin{aligned} C_2 \prod_{j=2}^{n-1} \tilde{\nu}_j - C_1 \prod_{j=1}^{n-1} \tilde{\nu}_j + C_0 \left[\alpha_{u-1}^{(r)} \right]^2 \prod_{j=2}^{n-1} \tilde{\nu}_j &= 0 \\ C_1 \prod_{j=1}^{n-1} \tilde{\nu}_j - C_0 \prod_{j=0}^{n-1} \tilde{\nu}_j &= 0 \end{aligned}$$

Then with the terminating conditions $C_1 = C_0 \tilde{\nu}_0$ and $C_0 = 1$, we can sum up the equations to eliminate the middle terms and obtain

$$C_n - Q_{0,n-1} + \sum_{j=0}^{n-2} (j+1) C_j \alpha_{u-(j+1)}^2 Q_{j+2,n-1} = 0$$

where we use a shorthand notation

$$Q_{0,n-1} = \prod_{j=0}^{n-1} \tilde{\nu}_j.$$

To find the analytical expression for C_n , we recursively expand the factor C_j

$$\begin{aligned} C_n &= Q_{0,n-1} - \sum_{j=0}^{n-2} (j+1) C_j \alpha_{u-(j+1)}^2 Q_{j+2,n-1} \\ &= Q_{0,n-1} - \sum_{j=0}^{n-2} Q_{0,j-1} Q_{j+2,n-1} (j+1) \alpha_{u-(j+1)}^2 \\ &\quad + \sum_{j=0}^{n-2} \sum_{k=0}^{j-2} Q_{j+2,n-1} Q_{0,k-1} Q_{k+2,j-1} \\ &\quad \times \left[(j+1) \alpha_{u-(j+1)}^2 \right] \left[(k+1) \alpha_{u-(k+1)}^2 \right] - \dots \end{aligned}$$

By observing that $Q_{0,j-1} Q_{j+2,n-1} = Q_{0,n-1} / \tilde{\nu}_j \tilde{\nu}_{j+1}$ and so on for each pair of Q 's in the terms of each recursive expansion, we can recursively factorize out $Q_{0,n-1}$ and arrive at

$$C_n = Q_{0,n-1} \sum_{p=0}^{\lfloor n/2 \rfloor} (-1)^p \sum_{\langle j_1 \dots j_k \dots j_{\lfloor n/2 \rfloor} \rangle} \dots \sum_{k=1}^p \frac{(j_k+1)}{\tilde{\nu}_{j_k} \tilde{\nu}_{j_k+1}} \left[\alpha_{u-(j_k+1)}^{(r)} \right]^2$$

where $\langle j_1 \dots j_k \dots j_{\lfloor n/2 \rfloor} \rangle$ is the index set described in Sec. IV. Finally, substituting the above expression back to the transformation Eq. (C4), we can obtain the coefficients of the excitation eigenvector as in Eq. (21).

2. One-excitation spectrum for a 4-qubit superconducting qubit chain

The state vector for the one-excitation 4-qubit SQC ($u=1$, $r=2$, and $m \in \{-2, -1, 0, 1\}$) can be written as

$$|u, r\rangle = c_0 |0; 2, 1\rangle + c_1 |1; 2, 0\rangle + c_2 |2; 2, -1\rangle + c_3 |3; 2, -2\rangle.$$

If we assume $c_0 = 1$ as a common factor, the rest three coefficients can be written as

$$\begin{aligned} c_1 &= R^{-1/2} \mathcal{C}_{1,0} \\ c_2 &= R^{-1} \mathcal{C}_{2,0} - \mathcal{C}_{2,1} \\ c_3 &= R^{-3/2} \mathcal{C}_{3,0} - R^{-1/2} \mathcal{C}_{3,1}. \end{aligned}$$

After plugging in the expression according to Eq. (22), we obtain the expressions shown in Table. I.

To find ν , and hence the excitation energy, consider the difference equations

$$\begin{aligned} C_4 - C_3 \tilde{\nu}_3 + 3C_2 (\alpha_{-2}^{(2)})^2 &= 0 \\ C_3 - C_2 \tilde{\nu}_2 + 2C_1 (\alpha_{-1}^{(2)})^2 &= 0 \\ C_2 - C_1 \tilde{\nu}_1 + C_0 (\alpha_0^{(2)})^2 &= 0. \end{aligned}$$

Since $C_4 = 0$ and $C_1 = \tilde{\nu}_0 C_0$, we derive from the last equation

$$C_2 = C_0 \left[\tilde{\nu}_0 \tilde{\nu}_1 - (\alpha_0^{(2)})^2 \right]$$

and from the first equation

$$C_3 = 3C_0 \left[\tilde{v}_0 \tilde{v}_1 + (\alpha_0^{(2)})^2 \right] \frac{(\alpha_{-2}^{(2)})^2}{\tilde{v}_3}.$$

Substitute these expressions into the second equation and with Eq. (16), we have

$$12(\tilde{v}_0 \tilde{v}_1 + 6R_{N,l})R_{N,l} - (\tilde{v}_0 \tilde{v}_1 - 6R_{N,l})\tilde{v}_2 \tilde{v}_3 + 12R_{N,l}\tilde{v}_0 \tilde{v}_3 = 0.$$

Expanding the \tilde{v} , we arrive at a fourth-order polynomial equation

$$v^4 - 6\tilde{\omega}_0 v^3 + [11\tilde{\omega}_0^2 - 30R_{N,l}\eta^2] v^2 - 6[\tilde{\omega}_0^3 - 13\tilde{\omega}_0 R_{N,l}\eta^2] v - 36R_{N,l}\eta^2 [\tilde{\omega}_0^2 + 2R_{N,l}\eta^2] = 0.$$

If we consider the case with $\tilde{\omega}_0 = 0$ (the conventional TC-model case), we have

$$v^4 - 30R_{N,l}\eta^2 v^2 - 72R_{N,l}^2 \eta^4 = 0$$

and the roots are

$$v = \pm \sqrt{(15 + 3\sqrt{33})R_{N,l}\eta}$$

On the other hand, if we consider a weak coupling case $\tilde{\omega}_0 \gg \eta$, then the equation becomes

$$v^4 - 6\tilde{\omega}_0 v^3 + 11\tilde{\omega}_0^2 v^2 - 6\tilde{\omega}_0^3 v - 36R_{N,l}\eta^2 \tilde{\omega}_0^2 = 0$$

and the solutions are

$$v = \frac{3}{2}\tilde{\omega}_0 \pm \frac{1}{2}\sqrt{5\tilde{\omega}_0^2 \pm 4\tilde{\omega}_0\sqrt{\tilde{\omega}_0^2 + 36R_{N,l}\eta^2}}.$$

Hence, the excitation energy can be written as in Eq. (23).

Now the coefficient c_1 for the highest eigenenergy state is, since usually $\tilde{\omega}_0 < 0$,

$$c_1 = \frac{v}{\sqrt{6R_{N,l}\eta}} = \frac{3}{2}\Omega + \frac{1}{2}\sqrt{5\Omega^2 - 4\Omega\sqrt{\Omega^2 + 6}}$$

where $\Omega = \tilde{\omega}_0/(\eta\sqrt{6R_{N,l}})$. Since $R_{N,l} \leq 1$,

$$|\Omega| \geq \left| \frac{\tilde{\omega}_0}{\sqrt{6}\eta} \right|$$

which means that the deformation leads to a larger coefficient c_1 than that of the undeformed case. For c_2 , we have

$$c_2 = \frac{1}{\sqrt{2}}(c_1^2 - \Omega c_1 + 1) > \frac{1}{\sqrt{2}}(c_1 + 1)^2$$

since $\tilde{\omega}_0 \gg \eta$ and so $|\Omega| \gg 2$. This means that c_2 increases by a greater proportion than c_1 due to the deformation. Similarly c_3 increasing by an even larger factor. The change in the coefficients shows that the a larger deformation favors the states with larger number of photons and a more ordered spin-chain.

-
- [1] J. Q. You and F. Nori, Phys. Rev. B **68**, 064509 (2003); J. Q. You, J. S. Tsai, and F. Nori, Phys. Rev. B **68**, 024510 (2003).
- [2] A. Blais, R.-S. Huang, A. Wallraff, S. M. Girvin, and R. J. Schoelkopf, Phys. Rev. A **69**, 062320 (2004).
- [3] J. Hauss, A. Fedorov, C. Hutter, A. Shnirman, and G. Schön, Phys. Rev. Lett. **100**, 037003 (2008).
- [4] H. Ian, Y.-X. Liu, and F. Nori, Phys. Rev. A **81**, 063823 (2010).
- [5] S. N. Shevchenko, S. Ashhab, and F. Nori, Phys. Rep. **492**, 1 (2010).
- [6] J. Q. You and F. Nori, Nature **474**, 589-597 (2011).
- [7] C. M. Wilson, G. Johansson, A. Pourkabirian, M. Simoen, J. R. Johansson, T. Duty, F. Nori, and P. Delsing, Nature **479**, 376 (2011).
- [8] J. Q. You and F. Nori, Phys. Today **58**, 42 (2005).
- [9] Y.-X. Liu, C. P. Sun, and F. Nori, Phys. Rev. A **74**, 052321 (2006).
- [10] F. Helmer, M. Mariantoni, A. G. Fowler, J. von Delft, E. Solano, and F. Marquardt, Europhys. Lett. **85**, 50007 (2009).
- [11] I. Buluta, S. Ashhab, and F. Nori, Rep. Prog. Phys. **74**, 104401 (2011).
- [12] A. L. Rakhmanov, A. M. Zagoskin, S. Savel'ev, and F. Nori, Phys. Rev. B **77**, 144507 (2008).
- [13] S. Savel'ev, V. A. Yampol'skii, A. L. Rakhmanov, and F. Nori, Rep. Prog. Phys. **73**, 026501 (2010).
- [14] J. M. Fink, R. Bianchetti, M. Baur, M. Göppl, L. Steffen, S. Filipp, P. J. Leek, A. Blais, and A. Wallraff, Phys. Rev. Lett. **103**, 083601 (2009).
- [15] Y.-D. Wang, F. Xue, Z. Song, and C.-P. Sun, Phys. Rev. B **76**, 174519 (2007).
- [16] N. Lambert, Y. Chen, R. Johansson, and F. Nori, Phys. Rev. B **80**, 165308 (2009).
- [17] P. Nataf and C. Ciuti, Phys. Rev. Lett. **104**, 023601 (2010).
- [18] L. Tian, Phys. Rev. Lett. **105**, 167001 (2010).
- [19] I. Buluta and F. Nori, Science **326**, 108 (2009).
- [20] I. Diniz, S. Portolan, R. Ferreira, J. M. Gérard, P. Bertet, and A. Auffèves, arXiv:1101.1842 (2011).
- [21] R. H. Dicke, Phys. Rev. **93**, 99 (1954).
- [22] A. P. Polychronakos, Mod. Phys. Lett. A **5**, 2325 (1990).
- [23] M. Roček, Phys. Lett. B **255**, 554 (1991).
- [24] C. Delbecq and C. Quesne, J. Phys. A **26**, L127 (1993).
- [25] D. Bonatsos, C. Daskaloyannis, and P. Kolokotronis, J. Phys. A **26**, L871 (1993).
- [26] G. D. Mahan, *Many particle physics* (Plenum Publishers, New York, 2000).
- [27] M. Tavis and F. W. Cummings, Phys. Rev. **170**, 379 (1968).
- [28] S. Swain, J. Phys. A **5** L3 (1972).
- [29] M. Reed and B. Simon, *Methods of modern mathematical physics* (Academic Press, San Diego, 1980).